Article

Hydrophilic Antimicrobial Coatings for Medical Leathers from Silica-Dendritic Polymer-Silver Nanoparticle Composite Xerogels

Michael Arkas [1,*], **Georgia Kythreoti** [1], **Evangelos P. Favvas**[1], **Konstantinos Giannakopoulos** [1], **Nafsica Mouti**[1], **Marina Arvanitopoulou**[1], **Ariadne Athanasiou**[1], **Marilina Douloudi**[1], **Eleni Nikoli**[1], **Michail Vardavoulias**[2] **Marios Dimitriou**[3], **Ioannis Karakasiliotis**[3,] **Victoria Ballén**[4] and **Sara M. Soto** [4]

[1] Institute of Nanoscience Nanotechnology, NCSR "Demokritos", Patriarchou Gregoriou Street, 15310 Athens, Greece; g.kythreoti@inn.demokritos.gr (G.K); e.Favvas@inn.demokritos.gr (E.F); k.giannakopoulos@inn.demokritos.gr (K.G); n.mouti@inn.demokritos.gr (N.M); marinaarva3@gmail.com (M.R); ariadne.a@hotmail.com (A.A.); marilina.douloudi@gmail.com (M.D.); e.nikoli@inn.demokritos.gr (E.N.).

[2] PYROGENESIS S.A., Technological Park 1, Athinon Avenue, 19500 Attica, Greece; mvardavoulias@pyrogenesis-sa.gr (M.V.).

[3] Laboratory of Biology, School of Medicine, Democritus University of Thrace, 68100 Alexandroupolis, Greece ioakarak@med.duth.gr (I.K); mardimitriou7@gmail.com {M.I.).

[4] ISGlobal, Hospital Clinic - Universitat de Barcelona, 08036 Barcelona, Spain; sara.soto@isglobal.org (S.S); victoria.ballen@isglobal.org (V.B).

* Correspondence: m.arkas@inn.demokritos.gr; Tel.: 0030 210 6503669

Abstract: Hybrid organic-inorganic (dendritic polymer-silica) xerogels containing silver nanoparticles (Ag-Nps) were developed as antibacterial leather coatings. The preparation method is environmentally friendly, based on two biomimetic reactions. Silica gelation and spontaneous (Ag-Np) formation were both mediated by hyperbranched poly (ethylene imine) (PEI) scaffolds of variable Mw (2000-750000). The formation of precursor hydrogels was monitored by dynamic light scattering (DLS). The chemical composition of the xerogels was assessed by Infra-Red Spectroscopy (IR) and Energy-dispersive X-ray spectroscopy (EDS) while the uniformity of the coatings was established by scanning electron microscopy (SEM). Release properties of coated leather samples and overall behavior in water in comparison to untreated analogs were investigated by UV-Vis spectroscopy. Antibacterial activity was tested towards *Escherichia coli*, *Pseudomonas aeruginosa*, and *Staphylococcus aureus*, and antibiofilm properties against *Staphylococcus aureus, Staphylococcus epidermidis, Escherichia coli, Acinetobacter baumannii, Enterococcus faecalis* while SARS-Cov-2 clinical isolate was employed for the first estimation of their antiviral potential. Toxicity was evaluated using the *Jurkat E6.1-cell line*. Finally, water contact angle measurements were implemented to determine the enhancement of the leather surface hydrophilicity caused by these composite layers. The final advanced products are intended for use in medical applications.

Keywords: dendrimers; hyperbranched; poly (ethylene imine); xerogels; antibacterial; SARS COVID-19 virus; antibiofilm; antiviral; water permeability; surface hydrophilicity

1. Introduction

The dendritic polymers derive from radial instead of the conventional linear polymerization [1] and are recognized as the fourth major macromolecular class alongside their linear, crosslinked, and branched analogs [2-7]. This flourishing class of macromolecules is characterized by a repetitive branched motif that governs their molecular and supermolecular structures. These unique architectures promote a repertoire of valuable properties for their applications as active ingredient carriers with potential for controlled release. Depending on the intended use, they are highly modifiable when it comes to their internal cores, branching points, and external functional groups [8-9] through the typical

synthetic procedures. Currently, there are five categories including the monodispersed symmetric dendrimers [10-12], the asymmetric hyperbranched polymers [13-16], fragments thereof, the [17-18], and finally the uncommon and complex dendronized polymers [19-21] and dendrigrafts [22].

In parallel to the research on dendritic polymers, the field of bioinspired nanoscience is also rapidly evolving as the need for materials with new and eco-friendly features is increasing. As a consequence, in many cases, the hybrid nanoparticles prepared, involve combinations of dendritic polymers with other materials, for instance, biomineralized metal nanoparticles [23] or biomimetically produced ceramics [24-26]. The unique physicochemical properties of these composites have made them ideal tools in everyday applications, such as additives in textiles [27], drug carriers [28], water purification agents [29], and heterogeneous catalysts [30]. Their production is considered to be environmentally friendly too, as it does not produce toxic byproducts, and does not require high temperatures or the use of toxic materials and solvents.

Among dendritic polymers, there is a special category presenting endogenous pharmaceutically activity. Hyperbranched poly (ethyleneimines) (PEIs) exhibit antibacterial activity and may operate in synergy with appropriate bactericides incorporated in their cavities [31]. These cationic polymers are hydrophilic and possess a high density of lone pairs. They can accommodate a large variety of molecules or ions, by thermodynamically favorable absorption through electrostatic or other intermolecular interactions and immobilize them through the formation of complexes, hydrogen, or conventional chemical bonds.

Ag-Nps are well-known antibacterial agents [32-36] and are selected as the active ingredient since silver has a sufficiently low reduction potential to undergo biomimetic mineralization in the PEI interior without additional reducing reagent (**Figure 1**). The commercial mixture (C8 to C18) of quaternary ammonium salts of alkyl benzyl dimethyl ammonium chloride (BAC) was chosen as a synergistic bactericidal reagent. It is also a cationic microbicide and exhibits a wide range of antimicrobial properties against bacteria, fungi, and viruses. It has been used as a bactericidal since 1935 [37], as a preservative for ophthalmic solutions since 1979 [38], and is widely used in the textile industry as an insecticide or antimicrobial [39-40]. It is extremely effective against the most important viruses: common flu, measles, rabies, herpes simplex, yellow fever, Venezuelan equine encephalitis, Japanese encephalitis B, adenovirus type 7, and meningitis [41].
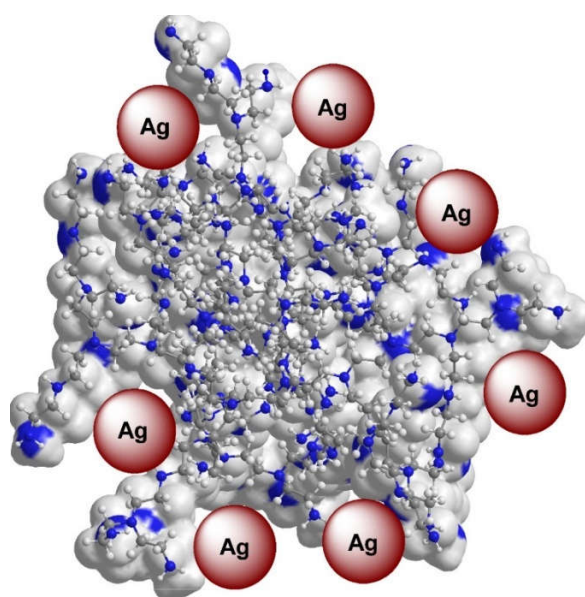
Figure 1. Schematic representation of Ag Nps nucleation inside the cavities of hyperbranched PEI.

On the outer surface of PEIs, the functional primary amino groups are capable of interacting with the appropriate reagents. They are ideal scaffolds for biomimetic silicification by the formation of complementary hydrogen bonds with orthosilicic acid, producing ceramics and gels. Hydrogels have many applications, as stationary phases in column chromatography, pharmaceuticals, desiccants, food additives moisture indicators, and carriers of active ingredients with controlled-release capabilities. [42-43]. The gentle dehydration-drying of silanol groups into siloxanes (**Figure 2**) affords silica xerogels. These versatile, materials are non-toxic and biocompatible [44-45]. They are more appropriate for carrying sensitive active ingredients for instance those susceptible to oxidation due to the very limited water content. Moreover, the applicability of high Mw (25,000-750,000) hyper-branched PEIs in living organisms is very limited due to their toxicity. Coupling with negatively charged orthosilicic acid neutralizes the large topical positive charge concentrations which is the main cause of the adverse side effects [46-47].
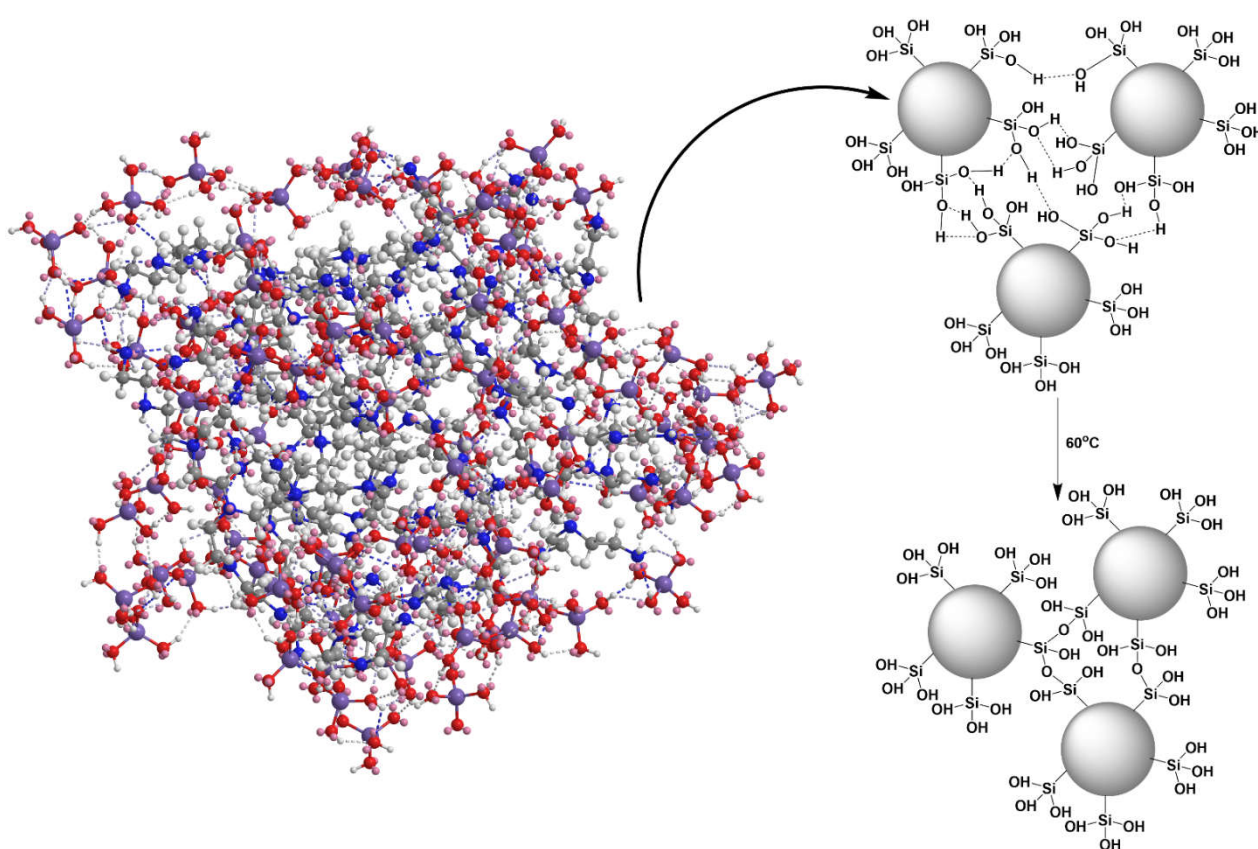
Figure 2. Schematic representation of the hydrogen bonding network formation around hyper-branched PEI and the transformation of silanols to siloxanes during the drying of hydrogels to xerogels.

The raw leather undergoes a chemical treatment, called tanning that provides permanent antisepsis and long-term resistance to bacteria & fungi. After drying special coatings are applied to the surface during the finishing process [48]. In the current work, we aim to develop a supplementary or to some extent alternative method for medical leather processing technology. Hybrid nanocomposite xerogels, composed of silica hyper-branched PEIs, Ag Nps, optionally carrying BAC as an additional antibacterial ingredient are employed as coatings. The application is done by wetting the leather surface with the gel-forming solution. During the solidification (coagulation) into the network of the pores, the agglomerates swell dramatically due to the intermolecular hydrogen bonds, and the solid layer is mechanically anchored to the leather. The desired properties include antibacterial, antiviral, and antibiofilm protection and enhanced hydrophilicity. The latter

facilitates subsequent incorporation of water-soluble components such as the BAC to the leather surface, The preparation method is environmentally friendly, based on two biomimetic reactions. Silica gelation and Ag-Np formation are both governed by the dendritic polymer.

2. Materials and Methods

2.1. Materials

PEI 2,000 (Mw= 2,000) trade name: Lupasol PR8515, PEI 5,000 (Mw=5,000) trade name Lupasol G100, PEI-25,000 (Mw= 25,000) trade name: Lupasol WF, PEI-750,000 (Mw= 750,000), trade name: Lupasol P, were purchased by BASF. Silver nitrate (AgNO$_3$) Tetraethyl orthosilicate, (Si(OC$_2$H$_5$)$_4$), and ampicillin were obtained from Sigma-Aldrich, trizma base from Research Organics, and ACTICIDE® BAC 50 from Thor Company. All compounds were used without further purification. The solutions were prepared with Ultrapure water (18.2 M cm, Millipore Milli-Q system).

2.2. Instrumentation-Characterization

The formation of precursor hydrogels was monitored by Dynamic Light Scattering (DLS) employing an AXIOS-150/EX (Triton Hellas) with a 30 mW He–Ne laser emitting at 658 nm and an Avalanche detector at 90°. The composite silica-hyperbranched PEI-Ag-Nps xerogel coated leathers were characterized by Fourier transform infrared spectroscopy (FTIR) conducted on a Nicolet Magna-IR Spectrometer 550. The uniformity of the coatings was investigated by Scanning Electron Microscopy (SEM) with an FEI Quanta Inspect microscope with W (Tungsten) filament, Low Vacuum capabilities, and an EDAX accessory for Energy-dispersive X-ray spectroscopy (EDS). A Cary 100 UV–visible spectrophotometer was used for the monitoring of Ag particle formation and their diffusion from the leather substrate.

2.3. Pretreatment of raw bovine hides and conversion into leathers

Dry leather samples (crust leather), were used as substrates for coating with hybrid nanocomposite xerogels. They were prepared in small laboratory drums using typical leather manufacture procedures. The raw material was bovine hides, of Greek origin from the Macedonia region, preserved with salt with an average area of 40 sqft per hide.

Typical crust leather preparation procedure includes the stages of soaking, liming, deliming, bating, pickling, and tanning for the production of wet-blue leather and re-tanning, fatliquoring, and dyeing for the final production of crust leather. Leather tanning was performed using Chromium (III) sulfate ([Cr(H2O)$_6$]$_2$(SO$_4$)$_3$) as a tanning agent, followed by a typical chrome re-tanning procedure

2.4. Synthesis of Ag-Nps/silica-PEI xerogels and coating of leathers

2.4.1. Silver nanoparticles

To 4 solutions of hyperbranched PEIs, (50 ml) one for each Mw (2000, 5000, 25000, 750000) all corresponding to about 40 mM in primary and secondary amino groups 12,5 ml of AgNO$_3$ (0,1M) were added. Ag-Np formation was observed after about 1 hour by the light-yellow color of the solution that turns red-brown after 8 days. As previously, visible spectroscopy established the completion of silver nucleation [50].

2.4.2. Composite Xerogels and Coating

Gel forming solutions were prepared by mixing 1 ml of an orthosilicic acid solution (1M) produced from the hydrolysis of tetraethoxysilane by 5mM HNO$_3$ under stirring for 15 min and an equal quantity (1ml) of the previously prepared silver-hyperbranched PEI solutions. Their pH was adjusted to 7.5 with trizma base, then 100μL were drop-wise applied onto the surface of 2cm x 2cm leather substrates. In about 1 hour a solid layer formation was observed due to gelation and the coated samples were dried overnight in an

oven at 60°C to transform hydrogels into xerogels. This coating procedure was repeated once more. A series of leather samples were also treated with simple PEI Ag Nps solution i.e. with 1 ml of deionized water in the place of orthosilicic acid for comparison purposes.

2.5. Antibacterial Assessment of the PEI-Ag-Nps Solutions

Escherichia coli ATCC 25922, *Pseudomonas aeruginosa* ATCC 27853, and *Staphylococcus aureus* ATCC 29213 were used as model microorganisms. The bacteria were propagated in Luria-Bertani (LB) medium, incubated at 37°C overnight with shaking at 200rpm. The overnight bacterial cultures were diluted (10^5 CFU/ml) and plated onto sample treated LB-agar and the viable bacterial count was enumerated after incubation of the plates at 37°C for 16h. Ampicillin (50 mg/ml) treated LB-agar was used as growth inhibition control and untreated LB-agar was used as a 100% growth control, for all microorganisms.

Four different PEI-Ag-Nps samples were tested at gradient dilution concentrations, based on their primary and secondary amino group concentration, ranging from 1mM to 31.25μM. Controls worked as expected with no inhibition of growth visible at untreated LB-agar plated microorganisms and in the presence of 50 mg/ml ampicillin, all microorganisms presented inhibition of growth, as expected.

2.6. Disk-diffusion method

2.6.1. Antibacterial activity of Leather Samples.

Five leather coupon categories were tested; each of them underwent a different treatment. Four of them were coated with the four different composite xerogel compositions corresponding to the four MW of hyperbranched PEI as described in paragraph 2.4.2 PEI 2000, PEI 5000, PEI 25000, and PEI 750000. For the fifth group, a simple solution of PEI 25000 Ag Nps was applied (PEI 25000 Ag Nps sol.). Finally, a sixth sample was used for comparison purposes. The latter was prepared by applying 20μl of ampicillin (50mg/ml) on the surface of a sample coated with simple silica xerogel (i.e., without Ag Nps) prepared by 1 ml orthosilicic acid (1M) and 1 ml of pure water. The leather samples before testing were cut into squares (1cm x 1cm) and sterilized by UV exposure (λ= 254 nm) for 30 min (15 min each side). Examples of Gram-negative, *Escherichia coli* ATCC 25922 and *Pseudomonas aeruginosa* ATCC 27853, as well as Gram-positive bacteria, *Staphylococcus aureus* ATCC 29213, were chosen for this study.

All selected microorganisms were propagated in Luria-Bertani (LB) medium at 37°C with shaking at 200 rpm overnight. The bacterial overnight cultures were diluted in LB-Agar (0.8% w/v) to final densities ranging from 1×10^5 and 1×10^8 CFUs/ml and layered on LB Agar plates where pre-sterilized leather samples were placed in contact with the bacteria-containing agar. The plates were incubated overnight at 37 °C. Controls were performed by placing 20μl Ampicillin (50 mg/ml) and water in 7 mm diameter holes made in the agar with a cork borer as negative and positive controls of growth inhibition, respectively. After the incubation period, the diameters of growth inhibitory zones were evaluated. Controls worked as expected with no inhibition of growth visible at the water-treated controls and a 10 to 20 mm diameter halo being formed in the presence of 50 mg/ml Ampicillin, for both concentrations of all microorganisms.

2.6.2. Effect of BAC incorporation

Leather samples were coated with silica-PEI 25000-Ag Nps composite xerogels as described in the previous section and were cut in squares (0.5cm x 0.5cm). 100 μl of BAC 50% were drop-wise applied on their surface. They were dried overnight at 60°C and this wetting procedure was repeated once more. Finally, they were sterilized as above. Escherichia coli ATCC 25922 were propagated diluted in LB-Agar (0.8% w/v) to final densities ranging from 1×10^6 to 1×10^3 CFUs/ml. Controls were performed with 20μl of Ampicillin (50 mg/ml).

2.7. Antiviral performance

To assess the potential of composite xerogels against Covid-19 in comparison to control samples, a SARS-Cov-2 clinical isolate was used [50]. The antiviral test was conducted on one coated leather sample and a control sample, i.e., leather that did not contain silica PEI Ag Nps; the size of the sample surface was 2 cm × 2 cm. A culture of SARS-Cov-2 was prepared by growing the virus on VERO cells for 48 hours in D-MEM at 37 °C in a CO_2 incubator. Subsequently, after centrifugation at 12000 rpm on a benchtop centrifuge for further purification and removal of cell debris, the culture was tittered using TCID50 at 106 TCID50 mL^{-1} as previously described [51]. The concentration of viruses used for testing was 104 (TCID50 mL^{-1}). The virus suspension was spread uniformly and loaded onto the leather surfaces with a sterile cotton swab. The virus-inoculated samples were incubated at 37 °C for 15 min in stationary conditions. After incubation, virus samples were removed from the surface using a sterile cotton swab pre-soaked in fresh DMEM medium and transferred to tubes for centrifugation for 2 min at 12000 rpm. Following centrifugation, serial dilutions of the eluent were transferred to 96 well plates seeded with VERO cells at a confluency of 105 cells per well and TCID50 mL^{-1} was calculated for every sample.

2.8. Antibiofilm Activity

To determine the antibiofilm potential of PEI Ag Nps solutions and composite silica-PEI-Ag Nps xerogels, untreated leather samples, as well as leather samples wet by simple PEI-Ag Nps solutions or coated with the xerogels, were used. Briefly, the leather samples were placed in a 6-well cell culture plate and 4 mL of bacterial inoculum with a final concentration of 5×10^5 CFU/mL was added. The plates were incubated for 48 hours. After that, the supernatants were collected, and the leather samples were carefully washed with 1x PBS and sonicated to detach the adhering bacteria. Colony counting was then carried out. All the experiments were carried out in triplicate.

2.9. Water Contact Angle Measurements

Dynamic contact angle (CA) measurements between the water and leather surfaces took place using the Kruss DSA30S optical contact angle measuring instrument (Hamburg, Germany). The CA measuring instrument has a range of 180° for surface tension ranging from 0.01 to 2000 mN/m. A digital image followed by the calculated droplet's contact angle is recorded automatically by the Advance - Kruss software. The instrument provides remarkable reproducibility and high accuracy of the measurements. During the measurements at any equilibrium stage of system drop/surface, a calculated contact angle is recorded automatically.

2.10. In vitro cytotoxicity assay

The cytotoxicity of the xerogels was established using the Jurkat E6.1-cell line. Cells were maintained in RPMI-1470 media supplemented with 10% fetal bovine serum (FBS), penicillin, and streptomycin at 37 °C and 5% CO_2 atmosphere before testing. Jurkat cells were grown in 96-well tissue culture plates to a cell density of 104 – 105 cells/well. Concentrations of the samples ranging between 31.25 μg/mL and 2000 μg/mL were added to the wells and incubated for 24 h at 37 °C and 5% CO_2. After incubation, 50 μL XTT (Canvax, CA031) was added to each well and incubated for 4 h at 37 °C and 5% CO_2.

The absorbance was measured at wavelengths of 450-500 nm (signal absorbance) and 630-690 nm (background absorbance) using a microplate reader to obtain the normalized absorbance. This value was calculated by subtracting the background absorbance from the signal absorbance.

A = 450-500 nm (Test) – 450-500 nm (Blank) – 630-690 nm (Test)

A sigmoidal curve was obtained in the analysis, which is the result of the calculation via a four-point logistic function to estimate the half-maximal inhibitory concentration (IC50).

3. Results and Discussion

3.1. Synthesis and Characterization

Absorption of Ag^+ ions into the PEI cavities causes the formation of complexes of the type $[Ag(N(C_2H_4) xH_{3-x})_2]^+$ with primary, secondary, and tertiary amines (x = 1-3 respectively). The first metallic Ag nuclei are formed with the aid of ambient light which causes the very slow photolysis of these complexes. These nanoparticles absorb in the range of 420 nm due to the electron vibrations of the surface plasmons of Ag nanoparticles with sizes between 10-50 nm changing the solution color to light yellow and gradually as they grow to orange and finally dark brown [52].

The first step for producing silica xerogels containing Ag-Nps is to avoid the precipitation of insoluble silver salts from non-reduced silver ions, particularly silver chloride. Thus, the common tetraethoxysilane acid hydrolysis reagent: hydrochloric acid (HCl) must be replaced. Nitric acid (HNO_3), proved to be ideal for this case. Comparative kinetic monitoring by DLS (Figure 3a) at pH 5 (to delay gel formation) in a ratio of 2:1 orthosilicic acid to PEI-750000 solution revealed that the silica-PEI agglomerates had a larger size when HNO_3 is used whereas considerable coagulation hysteresis has been observed. Given that this time gap was not carried out at the typical gelation pH (7.5), it turned out that nitric acid met the requisites to replace HCl. Repeating the kinetic study at a ratio of 1:1 orthosilicic acid to PEI at different Mw (Figure 3b) showed that the silica-PEI agglomerates generally grow faster in the solutions of the smaller dendritic polymers. A third comparative DLS kinetic study performed on the same PEIs containing silver Nps (Figure 3c) indicated in all cases similar exponential growth as a function of time. However, the agglomerates' size is up to 5 times larger than their counterparts without silver.

The FTIR spectra of leather coated with silica xerogel along with the corresponding untreated counterpart are shown in Figure 3d. For comparison purposes, the respective bands of dendritic PEI 25000 and their assignment are summarized in Table 1. The IR spectrum of the simple leather is dominated by the peaks of its major protein, i.e., collagen. The two characteristic bands of C=O stretching (Amide I) and N-H bending / C-N stretching (Amide II) are present at 1649 and 1548 cm^{-1}, respectively together with the weak, wide absorption at 3080 cm^{-1} due to the harmonic N-H stretching vibration of amide II absorption. The broadband corresponding to the antisymmetric hydrogen-bonded N-H stretching vibration, at 3400 cm^{-1}, is integrated into the broadband due to the hydrogen bond network of C-OH and $C-NH_x$ groups of the collagen. The SiO-H groups of the coated sample that have not been transformed to siloxane groups also absorb in this area (3250 cm^{-1}). The stress and bending vibrations of Si-OH are located at 965-970 cm^{-1} and 550-560 cm^{-1} respectively as well as the sharp stretching band of non-hydrogen bonded SiO-H at 3750 cm-1. The other significant peaks are attributed to the CH_3/CH_2 stretching (2954-2854 cm^{-1}) and bending (1450 cm^{-1}) vibrations. The antisymmetric C-N stretch of the amines and the bending of the secondary OH groups are found at 1100 cm^{-1} whereas the corresponding symmetric C-N stretch and the bending of the primary OH groups are at 1030 cm^{-1}. The characteristic strong silica bands: Si-O-Si stretch (1054 cm^{-1}), bend (793 cm-1), and rock (443 cm^{-1}) are typically present in the spectrum of xerogel coated leather proving the successful coating of leather substrates by the xerogels.
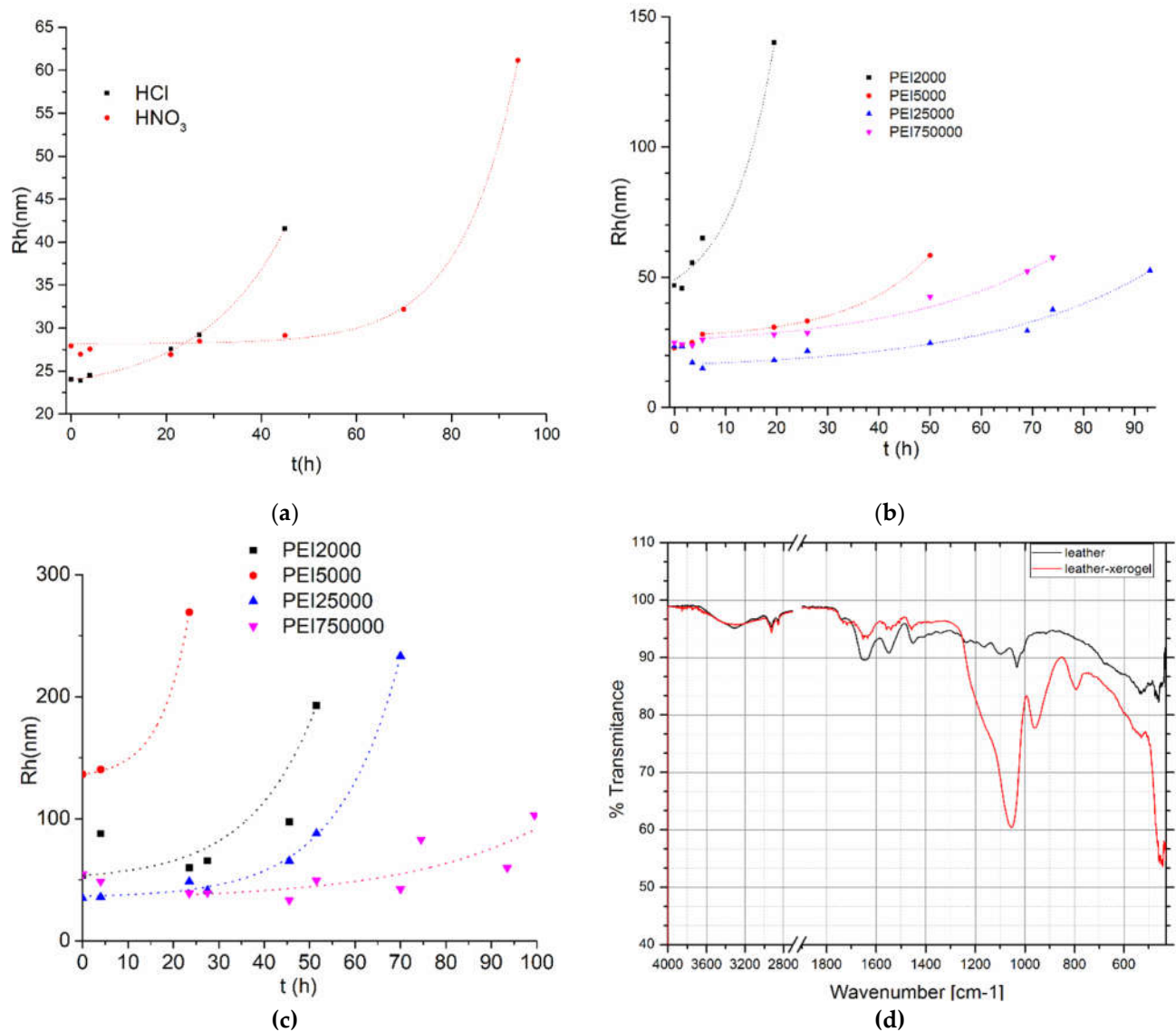
Figure 3. Size of agglomerates formed during gelation process **a.** PEI 750000 with tetra ethoxy silane hydrolyzed by HCl or HNO$_3$ **b.** Si(OH)$_4$-PEI and **c.** Ag Nps-Si(OH)$_4$-PEI-solutions as a function of time. **d.** IR spectra of uncoated leather (black) and a sample coated by Silica-PEI 25000-Ag Nps xerogel (red) exhibiting the characteristic silica bands.

Table 1. Assignment of the IR absorption bands of the uncoated leather; leather treated by silica-PEI 25000-Ag Nps and the hyperbranched poly(ethyleneimine) PEI 25000 (Mw 25000).

Band assignment	Collagen (Leather)	PEI-Silica-Leather	PEI-25000
ν_s SiO-H free	-	3750 (vw)	-
ν_{as} NH (primary-secondary)	op	3400 (w)	3350 (m)
ν_s NH (primary-secondary)	op	op	3276 (m)
ν NH OH (primary secondary hydrogen-bonded)	3294 (b)	3281(w/b)	
ν_s SiO-H Hydrogen bonded	-	3281 (w/b)	-
ν NH overtone of the amide II absorption	3080 (w/b)	op	-
ν_{as} CH$_3$	2954 (w)	2954 (w)	-
ν_{as} CH$_2$	2924 (m)	2924 (vw)	2935 (m)
ν_s CH$_3$	2868 (w)	2868 (w)	-
ν_s CH$_2$	2854 (s)	2854 (vw)	2810 (s)
ν C=O (Amide I) and Amide II of primary amides	1649 (s)	1649 (s)	-
δ NH, NH$_2$	-	op	1585 (m)
Amide II of secondary amides	1548 (m)	1548 (vw)	-
δ CH$_2$, CH$_3$	1451 (m)	1457 (m)	-
ν_s *C-O*	1341 (w)	op	-
ν_{as} C-N	1097 (s)	op	1105(m)
δ OH of secondary alcohols	1097 (s)	op	-
ν Si-O-Si	-	1054 (s)	-
δ OH of secondary alcohols	1032 (m)		
ν_s C-N	1032 (m)	op	1045 (m)
ν Si-O-Si	-	1054 (s)	-
ν Si-OH, Si-O$^-$	-	960 (m)	-
δ Si-O-Si	-	793(m)	-
δ Si-OH	-	530 (m)	-
ρ Si-O-Si	-	443 (s)	-

* a Assignments: ν (stretch), δ (bend), ϱ (rock). Subscripts as and s denote asymmetric and symmetric vibrations, respectively. Band intensities: s (strong), m (medium), w (weak) vw (very weak). sh (shoulder); br (broad). op (overlapped).

Figure 4 summarizes the SEM micrographs of treated and untreated leather samples. The pores are easily distinguished on the dark grey surface of raw leather (orange arrow **Figure 4a**). Using gel precursor solutions with high content in silica, one-step coating procedures, or drying abruptly under vacuum results in inhomogeneous coating and introduces cracks to the xerogels (**Figure 4b**). The orthosilicic acid / PEI AgNps 1:1 ratio combines much more uniform gel layers, reasonable coagulation times, and suitable viscosity of the gel-forming solution to penetrate the pores. A gentle drying at 60°C contributes to the result depicted in **Figure 4c**. Furthermore, a change in the surface color to a lighter grey (and even in lower voltage) is the first indication of a surface with increased polarity. Clusters and even some separate Ag Nps in the order of 10-20 nm are visible at higher magnifications (**Figure 4d**).
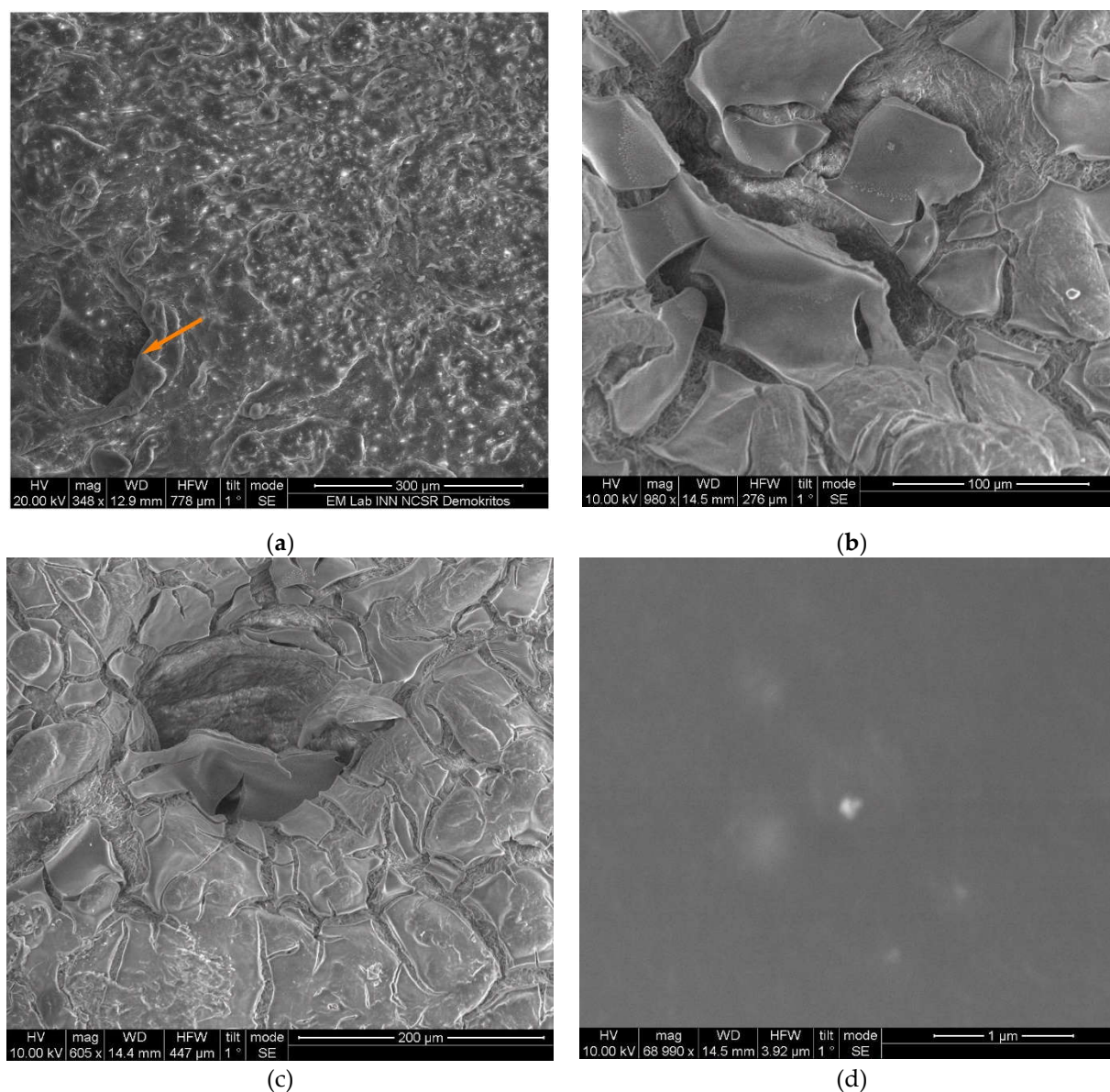
Figure 4. a. SEM micrograph of uncoated leather **b.** SEM micrograph of leather coated in a single-stage **c.** SEM micrograph coated in multiple stages indicating the penetration of the xerogel into the leather pores **d.** Ag nanoparticles incorporated into the xerogels.

The peaks in the Energy dispersive X-ray spectrum of untreated leather correspond to the posterior treatment stages that converted raw bovine hides to leather. Sodium and Chlorine originate from the NaCl used for preservation and Na_2S used for the denaturation of interfibrillar proteins; calcium from the $Ca(OH)_2$ that is employed in the alkaline swelling of the skin for the stabilization of the collagen fibers during the liming process. Aluminum and Silicon derive from kaolinite used during bating and Chromium and sulfur from the tanning agent ($[Cr(H_2O)_6]_2(SO_4)_3$). In parallel peaks corresponding to the natural organic components of the raw skin (C, N, O) are also present (**Figure 5a**). The incorporation of Ag Nps after wetting of the leather coupons with the PEI Ag Nps solution (**Figure 5b**) or coating by the composite xerogel (**Figure 5c**) was confirmed by the presence of AgLl, AgLa, AgLb, and AgLg peaks. In the latter case, the formation of SiO_2 is established by the dramatic increase of Si Ka and O Ka peaks. Finally, a small increase in the N peak is attributed to the nitrogen-rich PEI.

To get the first insight on the diffusion of silver nanoparticles; single or in conjunction with PEI to aquatic environments, leathers wet with PEI Ag Nps solution or coated by

hybrid xerogels were immersed in water. Kinetic UV-Vis monitoring of the absorption of the supernatants was performed by employing the supernatant of the untreated leather as a control (**Figure 5d**). As is evidenced by the spectra neither Ag NPs nor PEI release was observed in the positive absorption area of the spectra proving firm attachment of the hybrid layers to the leather substrate. Surprisingly the clearly defined peaks were directed downwards indicating negative absorption with constantly diminishing values. This means that the supernatant of the coated xerogels is poorer on these components than that of the untreated leather. Thus, xerogels have an unexpected beneficial effect in preserving the initial leather composition during washing. This phenomenon is carried out in the samples wet by the PEI-Ag Nps solution but to a much lesser extent. It seems thus that PEIs and their cavities also inhibit by themselves the leakage of the leather's compounds. Ag Nps diffusion, in this case, is minimal.


(a)

(b)

(c)

(d)
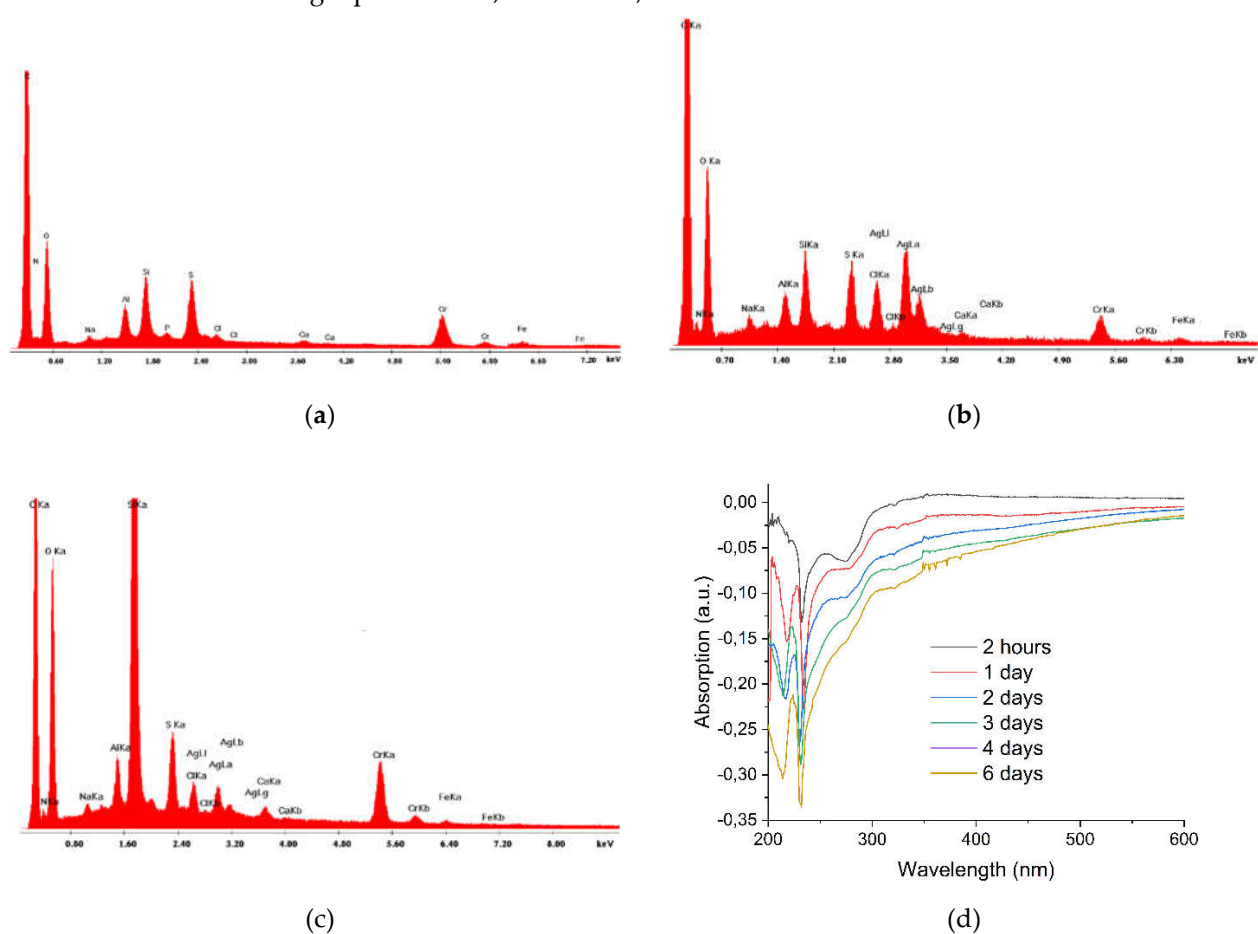
Figure 5. Energy-dispersive X-ray spectra of **a.** untreated leather **b.** leather wet with PEI AgNps **c.** leather coated by silica-PEI-Ag Nps composite xerogel **d.** UV-Vis spectra of supernatant solutions of leathers coated with composite xerogels in different time intervals. Respective supernatants of untreated leathers are used as controls.

3.2. Antimicrobial Assessment

3.2.1. PEI-Ag Nps Solutions

Overall, growth inhibition was observed for all PEI-Ag Nps solutions against all organisms (**Figure 6, Table 2**). Therefore, Ag Nps retain their antibacterial properties within the cavities of all PEIs (2000, 5000 25000, and 750000). In addition, all tested microorganisms, both Gram-positive and Gram-negative, presented susceptive to Ag solutions. In comparison, PEI 25000 presented the most effective inhibitory action against all microorganisms, with very low concentrations, followed by PEI 75000. PEI 5000 and PEI 2000 inhibit the growth of all three microorganisms, at higher concentrations.
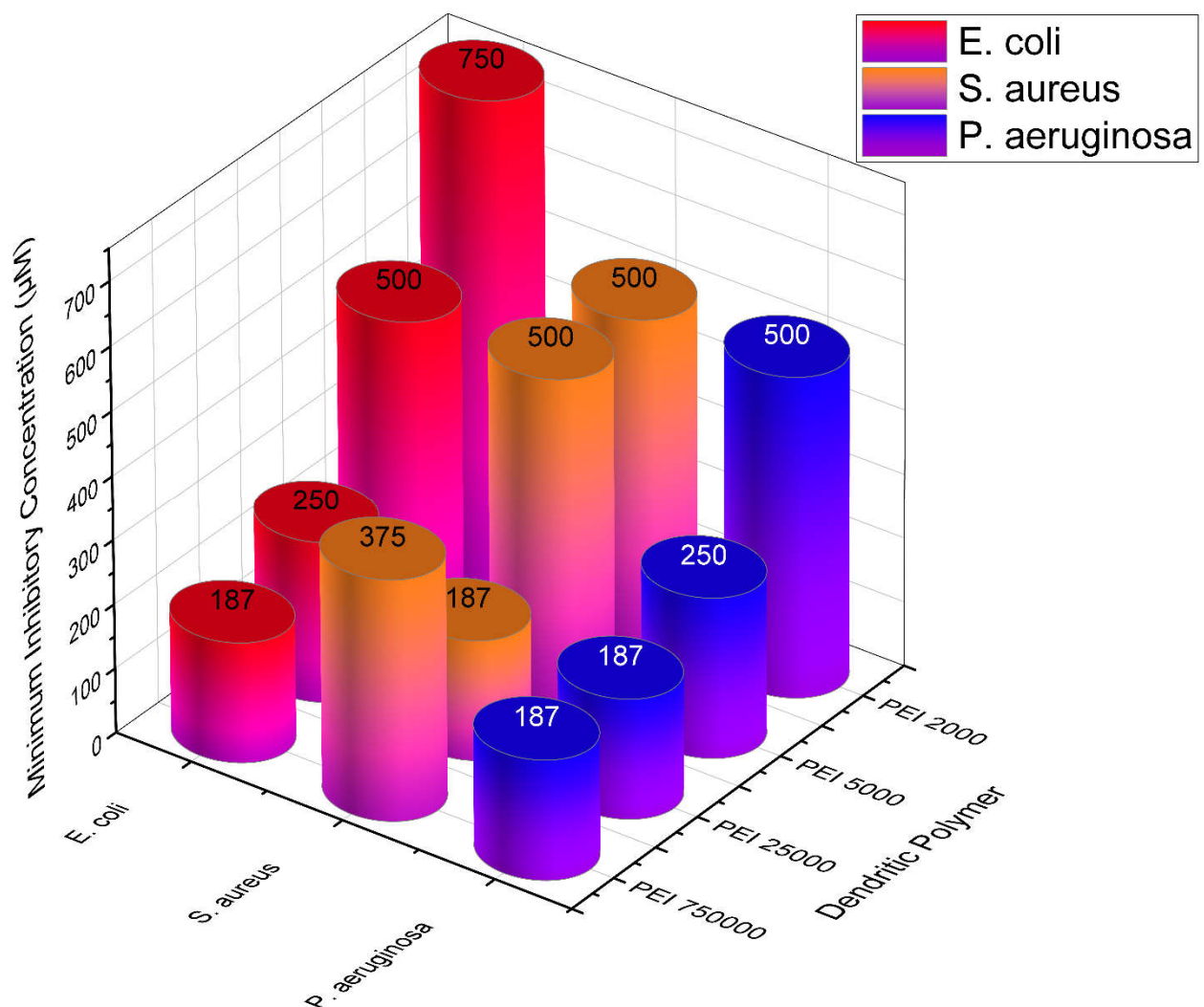
Figure 6. Minimum Inhibitory Concentrations (MIC) for all PEI Ag Nps concentrations tested for model Gram-negative microorganisms *Escherichia coli* ATCC 25922 and *Pseudomonas aeruginosa* ATCC 27853, and Gram-positive *Staphylococcus aureus* ATCC 29213.

Table 2. Results for PEI microbial minimum inhibitory concentrations.

Microorganism	PEI 2000	PEI 5000	PEI 25000	PEI 750000
E. coli ATCC 25922	750 μM	500 μM	250 μM	187 μM
S. aureus ATCC 29213	500 μM	500 μM	187 μM	375 μM
P. aeruginosa ATCC 27853	500 μM	250 μM	187 μM	187 μM

3.2.2. Antibacterial Performance of Ag Nps on the Leathers

As presented in **Table 3** and **Figures 7a, 7b** below, at *E.coli* 1 x 10^5 CFUs/ml concentration, all samples presented active with resulting halo diameters ranging from 3 to 5 mm, with the ampicillin treated leather sample resulting in a 12 mm halo diameter. Halo diameters presented here, are visible diameters of growth inhibition that are being formed outside the boundaries of the leather samples. At a higher bacterial concentration (1 x 10^8 CFUs/ml) only the 750000 and the ampicillin-treated samples presented halo formation outside the boundaries of the samples, 1 mm and 5 mm respectively, but no bacterial growth was visible on the leather-treated samples themselves.

Similar activities were observed for *S. aureus*, at 1 x 10^5 CFUs/ml concentration halo diameters ranging from 1 – 4 mm were observed, with the ampicillin-treated leather sample resulting in a 10 mm halo diameter. No bacterial growth inhibition was observed

outside the boundaries of the samples at higher bacterial concentration, 1×10^8 CFUs/ml. The ampicillin-treated sample presented the same inhibition potency for *S. aureus* as for *E.coli*, 5 mm. The 1×10^5 CFUs/ml concentration of P. aeruginosa presented lower activities for all tested samples by comparison, with inhibition diameters ranging from 0 - 2 mm. Ampicillin treated sample also presented lower activity for both higher and lower bacterial concentrations, no halo and 4 mm respectively. Interestingly some activity was observed at the higher, 1×10^8 CFUs/ml, concentration for both PEI 25000 samples and PEI 25000 Ag Np sol., 1 and 2 mm respectively.

The behavior of leathers treated by PEI Ag Nps solutions and SiO_2-PEI-Ag Nps xerogels in the LB agar is similar to that in water. Ag Nps although effectively protected their leather hosts presented limited diffusion, they formed detectable halos, substantially smaller in comparison to the readily soluble ampicillin. Thus in this instance, there is a measurable release of the antibacterial Nps and as noticed in the kinetic experiments in water it is slightly larger in the PEI 25000 Ag Nps sol samples in comparison to the PEI 25000 xerogel analogs, (**Figure 7c, d**) It is also interesting to note the smaller leather color diffusion of the sample coated by xerogel compared to the sample that was treated with the PEI Ag Nps solution. Finally, there is a seeming contradiction of the PEI 2000 Ag Nps. They exhibit comparatively lower activity in solutions in contradistinction to the respective results when incorporated into the leathers. They are two explanations: the low molecular weight of the hyperbranched polymer permits bigger mobility. Furthermore, low Mw PEI-Ag Nps generally form hybrid silica composites with higher contents in silver in comparison to their higher Mw counterparts [49, 53].

Table 3. The extent of propagation inhibition of *Escherichia coli* ATCC 25922, *Pseudomonas aeruginosa* ATCC 27853, and *Staphylococcus aureus* ATCC 29213 in the presence of treated leather samples.

Leather Sample	10^5 CFU/ml			10^8 CFU/ml		
	E. coli	*S. aureus*	*P. aeruginosa*	*E. coli*	*S. aureus*	*P. aeruginosa*
PEI 2000 Ag Nps	0.5 cm	0.3 cm	0.2 cm	No halo	No halo	No halo
PEI 5000 Ag Nps	0.4 cm	0.1 cm	No halo	No halo	No halo	No halo
PEI 25000 Ag Nps	0.3 cm	0.2 cm	0.1 cm	No halo	No halo	0.1 cm
PEI 25000 Ag Nps sol.	0.4 cm	0.4 cm	No halo	No halo	No halo	0.2 cm
PEI 750000 Ag Nps	0.3 cm	0.3 cm	0.1 cm	0.1 cm	No halo	No halo
Ampicillin on Xerogel	1.2 cm	1 cm	1 cm	0.5 cm	0.5 cm	No halo

(a)   (b)

(c)   (d)
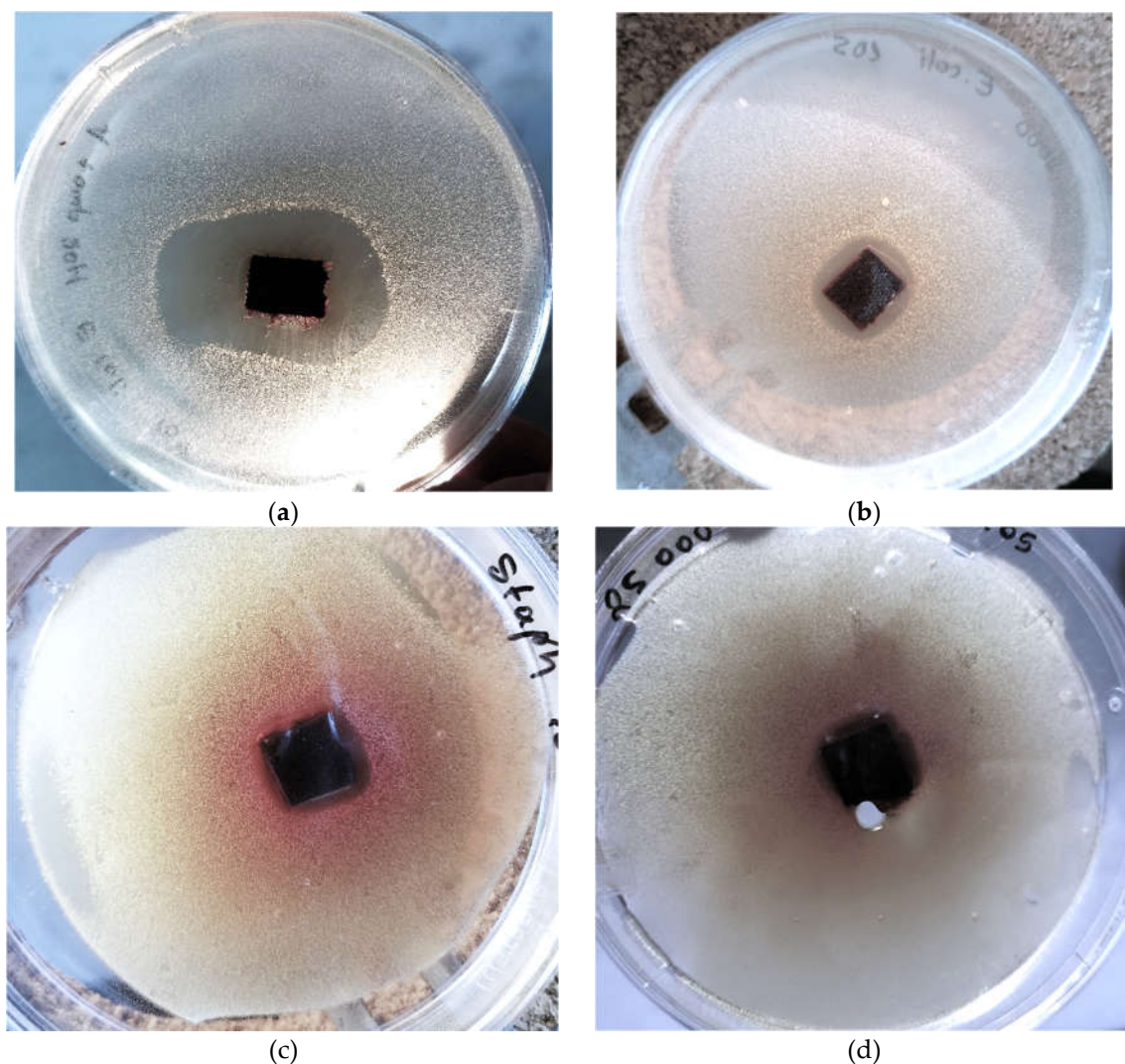
Figure 7. Representative examples of propagation inhibition of *Escherichia coli* ATCC 25922 from **a.** leather coated by silica PEI 25000-ampicillin xerogel, **b.** leather coated by silica PEI 2000 AgNps xerogel of *Staphylococcus aureus* ATCC 29213 from **c.** leather wet by PEI 25000 Ag Nps solution and **d.** silica PEI 25000 Ag Nps xerogel.

3.3. Cytotoxicity Test

The IC_{50} value provides information on the concentration required to inhibit a specific biological or biochemical process in vitro by 50%. The IC_{50} obtained for each xerogel is indicated in each graph (**Figures 8a-d**). PEI 25000 Ag Nps xerogel presents the highest toxicity that is comparable to that of the hyperbranched precursor [54-55]. This justifies in part its best bactericide performance and particularly the halos observed in leathers coated by PEI 25000 solution and xerogel and exposed in high concentration cultures of *Pseudomonas aeruginosa* ATCC 27853. Silica PEI 750000 AgNps xerogel despite the much higher MW of the precursor polymer is less toxic. Most probably the high local concentrations of ammonium cations are more effectively neutralized by the silanol groups of the ortho-silicic acid. Taking into account its, more than satisfactory, antibacterial performance it presents the best alternative solution. Nevertheless, since neither PEI nor silver nanoparticle release was detected in the kinetics experiments these toxicities do not present a major drawback.
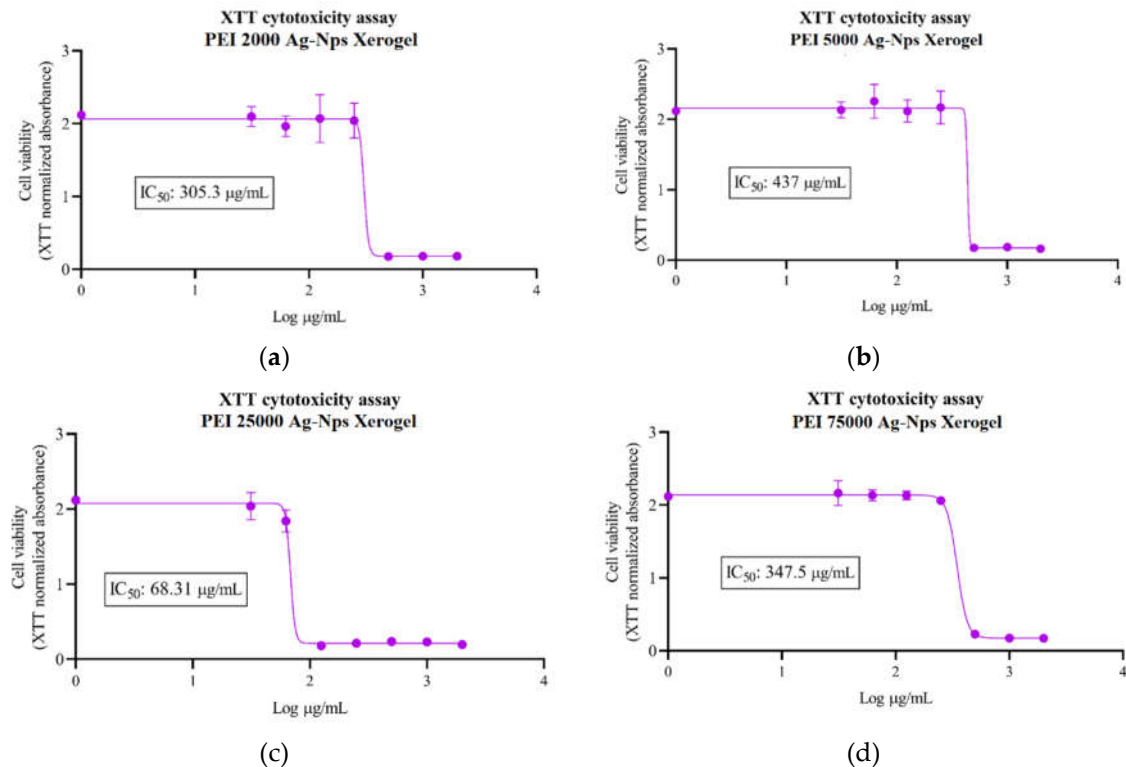
Figure 8. Cytotoxicity of the xerogels produced from hyperbranched PEI matrices of different Mw.

3.4. Antiviral performance

The xerogel composite coatings were also tested for their antiviral activity against SARS-CoV-2. The viability of SARS-CoV-2 was assessed for its ability to infect cells in culture under BSL3 conditions. coating of leather showed a 10-fold (*$p < 0.05$) reduction in virus titre as to uncoated leather (**Table 4**). This result is analogous to the activity obtained against SARS-CoV-2 (87 %) when polyester fabrics were printed with Selenium Nanoparticles [56] and close to those observed for spandex fabric coated with poly(Hexamethylene Biguanide) hydrochloride (PHMB) [57].

Table 4. Virus viability as measured using TCID50 on xerogel coated leather coupons in comparison to control leather samples. Statistical significance was performed using a t-test.

	TCID50/ml	
Microorganism	**Untreated Leather**	**Composite Xerogels**
SARS-COV-2	10000 ± 944	1000 ± 94.4

3.5. Antibiofilm activity of PEI-Ag Nps solutions and xerogels coatings on leather samples

We performed colony counts on both the supernatant and the leather samples (**Tables 5,6**). We observed that xerogels, as well as PEI Ag Nps solutions, inhibit bacterial growth when compared to controls, mainly with *S. aureus, S. epidermidis, E. coli,* and *E. faecalis*. However, we did not obtain growth of *A. baumanni*i in either the supernatant or the untreated leather samples. Additionally, *S. aureus* did not adhere to the untreated leather samples while the capacity of adherence of *S. epidermidis* was very low. In the case of *E. coli* and *E. faecalis*, the treatment of the leather using both composite xerogels and PEI Ag Nps solutions, inhibited the adherence of these strains, avoiding biofilm formation.

Table 5. Supernatants colony counts:.

Microorganism	CFU/cm²		
	Untreated Leather Samples	Composite Xerogels	PEI-Ag-Nps Solutions
Staphylococcus aureus	>300	1	25
Staphylococcus epidermidis	>300	0	0
Escherichia coli	>300	31	0
Acinetobacter baumannii	0	0	0
Enterococcus faecalis	>300	55	35

Table 6. Sonicated leather samples colony counts:.

Microorganism	CFU/cm²		
	Untreated Leather Samples	Composite Xerogels	PEI-Ag-Nps Solutions
Staphylococcus aureus	0	1	0
Staphylococcus epidermidis	3	0	0
Escherichia coli	>300	0	0
Acinetobacter baumannii	0	0	0
Enterococcus faecalis	>300	8	8

3.6. Surface and pore hydrophilicity – Water Permeability

The affinity of the leather samples to water was assessed by the equilibrium contact angle of three leather samples (untreated, treated twice by PEI-silver Np solution, and coated twice by silica PEI 750000 Ag Nps xerogels) through the contact angle measurement, as shown in **Table 7**. Contact angle decreases from raw leather sample to the PEI Ag Nps treated sample and finally to sample coated with xerogel. In specific, a non-wetting surface, hydrophobic, with a water contact of about 99° becomes a partial wetting surface after the treatment with PEI Ag Nps (WCA ~69°) and finally a fully wet surface in the case of composite xerogel layers.

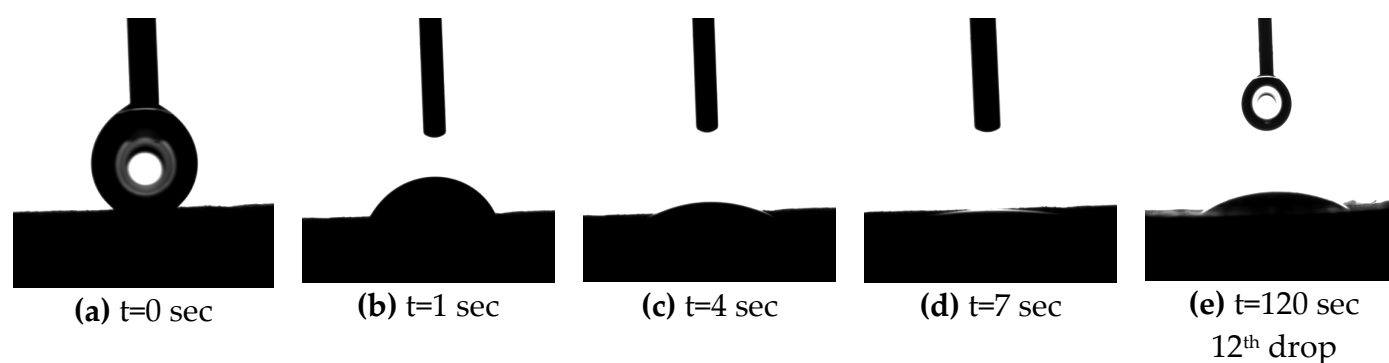**Table 7.** Water contact angle properties of the three studied leather samples.

Sample Name	Contact #1	Angle #2	Test #3	Average Value
Raw Leather	98.85	98.04	99.6	98.83
Leather PEI Ag Nps Solution	68.15	69.05	68.25	68.48
Leather-Composite Xerogels	-	-	-	full absorption of water

As is shown in **Figure 10a** the raw leather is characterized as a non-wetting surface, where the water drop can stay stable forming a contact angle of about 99°. The situation changes after the modification of the leather surface by PEI Ag NPs solution where the surface transformed to a partial wetting and the contact angle between the water drop and the surface decreases to about 68° (**Figure 10b**). This behavior has been also reported by other researchers. In specific, Štěpánová et al., who used chromium-tanned cow leather, used for leather shoe fabrication, show a reduction of water contact angle from 85° to 45° after 10 sec of plasma treatment [58]. In addition, acid-pickled bare pig skin was modified through O_2/H_2O low-temperature plasma treatment by Uou et al. [59] to change the wettability properties. With this treatment, a reduction of WCA was achieved from 84 to about 21°. These results are comparable with ours in the case of the sample treated with the PEI AgNps Solution. However, to our knowledge, there are no results in the literature comparable to the polarity of the sample coated with the silica xerogel. In this case, the wettability was enhanced dramatically and the surface became completely permeable to water, as is depicted in the snapshot images in **Figure 11**. Any drop which was deposited on the leather surface was absorbed into the material matrix until full saturation. The latter

occurred after the deposition of the 12th water drop (at the same surface area/point) and a required time of about 2 minutes.

(a)   (b)
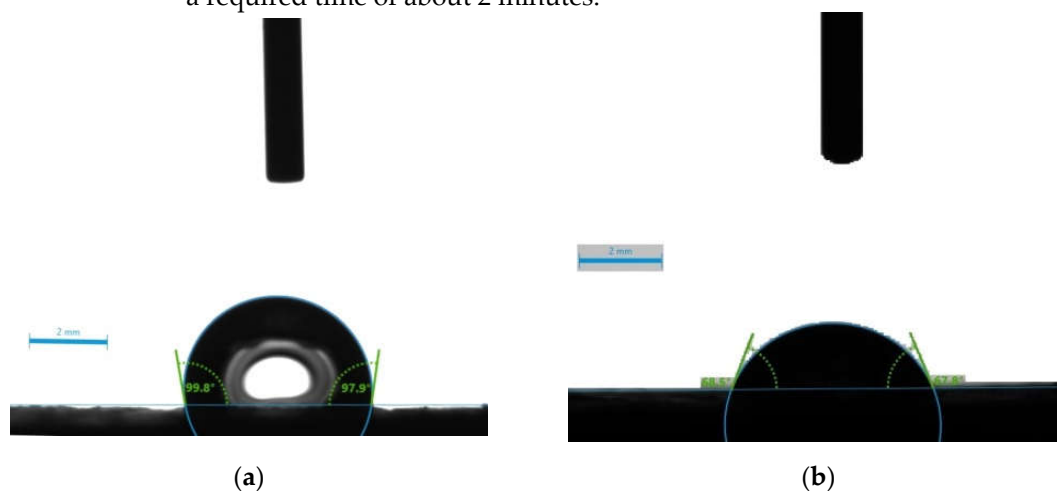
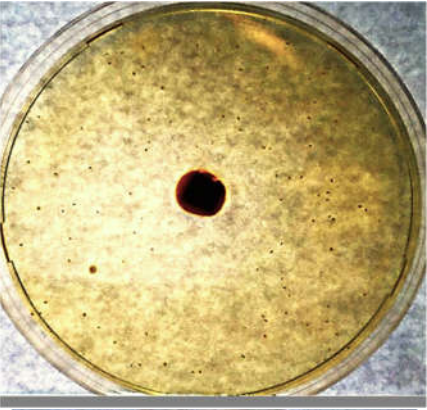**Figure 10.** Water contact angles of raw leather (a) and leather modified by PEI-Ag Nps solution (b).
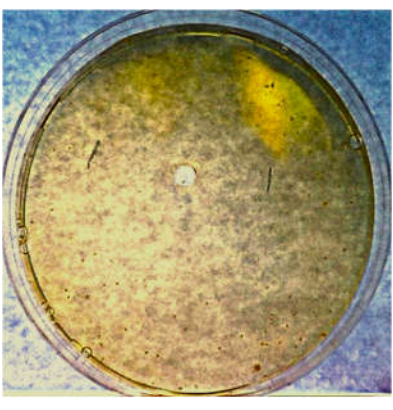

(a) t=0 sec   **(b)** t=1 sec   **(c)** t=4 sec   **(d)** t=7 sec   **(e)** t=120 sec
                                                                                                                           12th drop
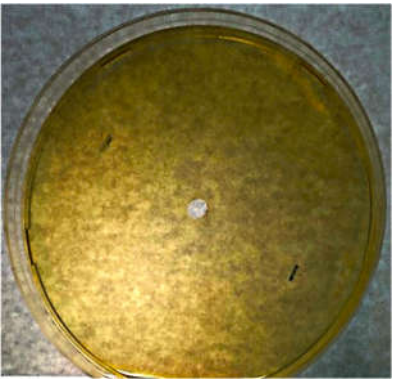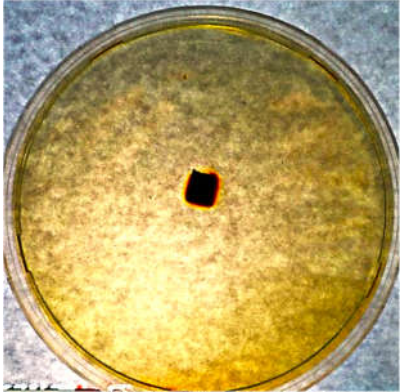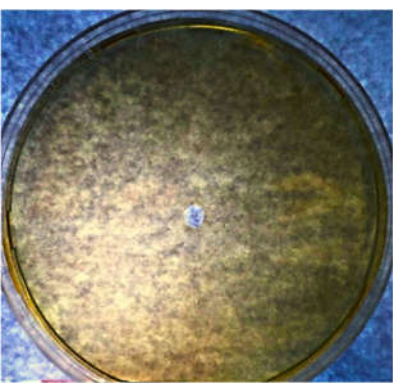
Figure 11. Water contact angles of leather coated by composite xerogels at different time intervals.

3.3 Antibacterial activity of leathers coated by composite xerogels bearing additional microbiocide agents.

To exploit the enhanced hydrophilicity of the xerogel layer, we performed an additional treatment with a water-soluble bactericidal. As a synergistic reagent, we chose the commercial mixture of quaternary ammonium salts of (C8 to C18) alkyl benzyl dimethyl ammonium chloride (BAC). This is a cationic microbicide that exhibits a broad spectrum of antimicrobial properties against bacteria, fungi, and viruses and is widely used in the textile industry as an insecticide or antimicrobial. [60-61]. At *E. coli* concentrations of 1×10^3 and 1×10^4 CFUs/ml, the antibacterial activities of the leather coatings were equivalent to pure ampicillin! (**Table 8**). At higher bacterial concentrations (1×10^5 and 1×10^6 CFUs/ml) the diameters of halos formed were 1-1.5 cm smaller than those of ampicillin (4 to 5 cm and 2.5 to 4 cm respectively). Thus, similarly, the composite hydrogels may host any polar active ingredient that will increase their activity, or provide additional properties and release capabilities.

Table 8. Luria-Bertani (LB) medium Agar plates bearing at the center leather samples (left) or 20 μl ampicillin (50 μg/ml) (right) incubated with different densities of *Escherichia coli* ATCC 25922 E cultures.

E.coli (CFU/ml)	PEI 25000 xerogel + BAC	Ampicillin [50 mg/ml]
1×10^6		
1×10^5		
1×10^4		
1×10^3		

4. Conclusions-Perspectives

Silica-dendritic PEI xerogel composites with Ag Nps optionally bearing BAC as an additional active ingredient provided antibacterial, antibiofilm, and antiviral, coatings to leathers. The gel formation reactions were performed in the pores of the substrate resulting in practical immobilization of the SiO_2 layer. Precursor solutions of hyperbranched PEIs with Ag Nps may as well present an adequate alternative with minimal metal release in aqueous solutions. The xerogels though increased dramatically the hydrophilicity of the surface rendering it susceptible to additional treatment with polar substances. Furthermore, they partially protected leather components from diffusion to water. Solution and gels produced with hyperbranched PEI 25000 presented the best results but also the highest toxicity. PEI 750000 is the best alternative since it combines satisfactory results with fewer side effects.

Gels with desired properties can be produced by using modified alkoxysilanes as silica precursors and their release properties may be fine-tuned by employing functionalized dendritic polymer(s). Other parameters may be altered such as the gelation pH (and the chemical compound used for the adjustment), the silica precursor to dendritic polymer solution ratio, or the metal of the nanoparticles, and result, in combination with a variety of active ingredients, in composites with specialized custom properties.

Apart from the disclosed coating method xerogels may form aqueous dispersions and be introduced to leathers by spraying. Titania (TiO_2) and Zinc Oxide (ZnO) may also be employed as the suspension base (substrate) to induce or enhance antiallergic properties. All these probabilities are very useful for the production of leathers employed in medical applications such as examination beds, leather medical shoes, ICU beds, surgical beds, leather anti-decubitus pillows, leather wheelchair lining, and leather hospital chairs.

5. Patents

M. Arkas, E.Nikoli, M. Douloudi,G. Kythreoti, L. Arvanitopoulos K. Arvanitopoulos Hydrogel and xerogel active ingredient carriers made from dendritic polymers and silica for use as leather and textile additives. Greek Patent eFiling Number 22-0003846572 26/11/2020.

References

1. J. M. J. Fréchet, D. A. Tomalia, Dendrimers and Other Dendritic Polymers, first ed., John Wiley & Sons, Ltd., Chichester, 2001.

2. Vögtle, F. Gestermann, S. Hesse, R. Schwierz, and H. Windisch, B. (2000). Functional Dendrimers. Prog. Polym. Sci., 25, pp. 987-1041. https://doi.org/10.1016/S0079-6700(00)00017-4.

3. Newkome, G. R. Moorefield, C.N. and Vögtle, F. (2001). Dendrimers and dendrons. Concepts, syntheses, perspectives.1st Ed. Weinheim: Wiley-VCH. https://doi.org/10.1002/3527600612.

4. Bosman, A. W. Janssen, H. M. and Meijer, E. W. (1999). About Dendrimers: Structure, Physical Properties, and Applications Chem. Rev., 99, pp. 1665-1688. https://doi.org/10.1021/cr970069y.

5. Lee, C. C. MacKay, J. A. Fréchet, J. M. J. and Szoka, F. C. (2005) Designing dendrimers for biological applications. Nature Biotechnol., 23, pp. 1517-1526. https://doi.org/10.1038/nbt1171.

6. Tomalia, D. A. and Fréchet, J. M. J. (2002). Discovery of dendrimers and dendritic polymers: a brief historical perspective. J. Polym. Sci. Part A Polym. Chem., 40, pp. 2719-2728. https://doi.org/10.1002/pola.10301.

7. Fréchet, J. M. J. Hawker, C. J. Gitsov, I. and Leon, J. W. (1996). Dendrimers and hyperbranched polymers: Two families of three-dimensional macromolecules with similar but clearly distinct properties. J. Macromol. Sci. Part A Pure Appl. Chem., 33, pp. 1399-1425. https://doi.org/10.1080/10601329608014916.

8. Arkas, M., Eleades, L., Paleos, C. M., & Tsiourvas, D. (2005). Alkylated hyperbranched polymers as molecular nanosponges for the purification of water from polycyclic aromatic hydrocarbons. Journal of applied polymer science, 97(6), 2299-2305. https://doi.org/10.1002/app.22026.

9. Allabashi, R., Arkas, M., Hörmann, G., & Tsiourvas, D. (2007). Removal of some organic pollutants in water employing ceramic membranes impregnated with cross-linked silylated dendritic and cyclodextrin polymers. Water Research, 41(2), 476-486.

10. Dvornic, P. R. and Tomalia, D. A. (1994). Starburst dendrimers – a conceptual approach to nanoscopic chemistry and architecture. Macromol. Symp., 88, pp. 123-148. Zeng, F. and Zimmerman, S. C. (1997).

11. Bosman, A. W. Janssen, H. M. and Meijer, E. W. Dendrimers in supramolecular chemistry: from molecular recognition to self-assembly. Chem. Rev., 97(7), 1681-1712. (1999). About Dendrimers: Structure, Physical Properties, and Applications Chem. Rev., 99, pp. 1665-1688.

12. Tully, D. C. and Fréchet, J. M. J. (2001). Dendrimers at surfaces and interfaces: chemistry and applications. J. Chem. Commun., 14, pp. 1229-1239.

13. Jikei, M. and Kakimoto, M.-A. (2001). Hyperbranched polymers: A promising new class of materials. Prog. Polym. Sci. (Oxford), 26(8), pp. 1233-1285.

14. Kim, Y.H. (1998). Hyperbranched polymers 10 years after. J. Polym. Sci. A1, 36(11), pp. 1685-1698.

15. Sunder, A. Heinemann, J. and Frey, H. (2000). Controlling the growth of polymer trees: Concepts and perspectives for hyperbranched polymers. Chem.-Eur. J., 6(14), pp. 2499-2506.

16. Yates, C.R. and Hayes, W. (2004). Synthesis and applications of hyperbranched polymers. Eur. Polym. J. 40(7), pp. 1257-1281.

17. Grayson, S.M. and Fréchet, J.M.J. (2001). Convergent Dendrons and Dendrimers: from Synthesis to Applications. Chem. Rev., 101(12), pp. 3819-3867.

18. Rosen, B. M. Wilson, C. J. Wilson, D. A. Peterca, M. Imam, M. R. and Percec V. (2009). Dendron-mediated self-assembly, disassembly, and self-organization of complex systems. Chem. Rev., 109(11), pp. 6275-6540.

19. Schlüter, A.D. and Rabe, J.P. (2000). Dendronized polymers: Synthesis, characterization, assembly at interfaces, and manipulation. Angew. Chem. Int. Edit., 39(5), pp. 864-883.

20. Frauenrath, H. (2005). Dendronized polymers - Building a new bridge from molecules to nanoscopic objects. Prog. Polym. Sci. (Oxford), 30(3-4), pp. 325-384. Chen, Y. and Xiong, X. (2010). Tailoring dendronized polymers. Chem. Commun. 46(28), pp. 5049-5060.

21. Zhang, A. (2005). Synthesis, characterization and applications of dendronized polymers. Prog. Chem., 17(1), pp. 157-171.

22. Teertstra, S.J. and Gauthier, M. (2004). Dendrigraft polymers: Macromolecular engineering on a mesoscopic scale. Prog. Polym. Sci. (Oxford), 29(4), pp. 277-327.

23. Arkas, M., Anastopoulos, I, Giannakoudakis, D. A., Pashalidis, I., Katsika, T., Nikoli, E., ... & Douloudi, M. (2022). Catalytic Neutralization of Water Pollutants Mediated by Dendritic Polymers. Nanomaterials, 12(3), 445. https://doi.org/10.3390/nano12030445.

24. Tsiourvas, D., Tsetsekou, A., Papavasiliou, A., Arkas, M., & Boukos, N. (2013). A novel hybrid sol-gel method for the synthesis of highly porous silica employing hyperbranched poly (ethylene imine) as a reactive template. Microporous and mesoporous materials, 175, 59-66. https://doi.org/10.1016/j.micromeso.2013.03.013.

25. Petrakli, F., Arkas, M., & Tsetsekou, A. (2018). α-Alumina nanospheres from nano-dispersed boehmite synthesized by a wet chemical route. Journal of the American Ceramic Society, 101(8), 3508-3519. https://doi.org/10.1111/jace.15487.

26. Kitsou, I., Arkas, M., & Tsetsekou, A. (2019). Synthesis and characterization of ceria-coated silica nanospheres: Their application in heterogeneous catalysis of organic pollutants. SN Applied Sciences, 1(12), 1-12. https://doi.org/10.1007/s42452-019-1613-y.

27. Martin, C. A., Lin, Z., Kumar, A., Dinneen, S. R., Osgood III, R. M., & Deravi, L. F. (2020). Biomimetic Colorants and Coatings Designed with Cephalopod-Inspired Nanocomposites. ACS Applied Bio Materials, 4(1), 507-513. https://doi.org/10.1021/acsabm.0c01034.

28. Esfand, R., & Tomalia, D. A. (2001). Poly (amidoamine)(PAMAM) dendrimers: from biomimicry to drug delivery and biomedical applications. Drug discovery today, 6(8), 427-436. https://doi.org/10.1016/S1359-6446(01)01757-3.

29.   Arkas, M., & Tsiourvas, D. (2009). Organic/inorganic hybrid nanospheres based on hyperbranched poly (ethylene imine) encapsulated into silica for the sorption of toxic metal ions and polycyclic aromatic hydrocarbons from water. Journal of hazardous materials, 170(1), 35-42. https://doi.org/10.1016/j.jhazmat.2009.05.031.

30.   Kitsou, I., Panagopoulos, P., Maggos, T., Arkas, M., & Tsetsekou, A. (2018). Development of SiO_2@ TiO_2 core-shell nanospheres for catalytic applications. Applied Surface Science, 441, 223-231. https://doi.org/10.1016/j.apsusc.2018.02.008.

31.   Parisi O. I., Scrivano L., Sinicropi. S., Puoci F., (2017). Polymeric nanoparticle constructs as devices for antibacterial therapy, Current Opinion in Pharmacology, 36, 72-77.

32.   Shameli K., Ahmad M. B., Jazayeri S. D., Shabanzadeh P., Sangpour P., Jahangirian H., Gharayebi Y., Investigation of antibacterial properties silver nanoparticles prepared via green method, Chem. Central J., 6, 2012, 73:1¬10.

33.   Jegatheeswaran S., Sundrarajan M., PEGylation of novel hydroxyapatite/PEG/Ag nanocomposite particles to improve its antibacterial efficacy, Mater. Sci. Eng. C 51 (2015) 174-181.

34.   C. Lok, C. Ho, R. Chen, Q. He, W. Yu, H. Sun, P.K. Tam, J. Chiu, C. Che, Proteomic analysis of the mode of antibacterial action of silver nanoparticles research articles, J. Proteome Res. 5 (2006) 916-924.

35.   J.S. Kim, E. Kuk, K.N. Yu, J.H. Kim, S.J. Park, H.J. Lee, S.H. Kim, Y.K.Park, Y.H. Park, C.Y. Hwang, Y.K. Kim, Y.S. Lee, D.H. Jeong, M.H. Cho, Antimicrobial effects of silver nanoparticles, Nanomed. Nanotechnol. Biol.Med. 3 (2007) 95-101.

36.   S. Jaiswal, P. McHale, B. Duffy, Preparation and rapid analysis of antibacterial silver, copper and zinc doped sol-gel surfaces, Colloids Surf. B: Biointerfaces 94 (2012) 170-176.

37.   Marple, B., P. Roland, and M. Benninger, 2003. Safety Review of Benzalkonium Chloride Used as a Preservative in Intranasal Solutions: An Overview of Conflicting Data and Opinions. American Academy of Otolaryngology-Head and Neck Surgery Foundation, Inc., USA., pp: 131-142.

38.   Gloor, M., B. Schorch and U. Hoeffler, 1979. The feasibility of replacing antibiotics by quaternary ammonium compounds in topical antimicrobial acne therapy. Arch. Dermato. Res., 265: 207-212.

39.   Kim, Y.H. and G. Sun, 2001. Durable antimicrobial finishing of nylon fabrics with acid dyes and a quaternary ammonium salt. Text. Res. J., 71: 318-323.

40.   Tatsuo, T., I. Masahiro, K. Kyoji and S. Yukio, 1989. Synthesis and antibacterial activity of copolymers having a quaternary ammonium salt side group. J. Applied Polymer Sci., 37: 2837-2843.

41.   J. A. Armstrong and E. J. Froelich, Inactivation of Viruses by Benzalkonium Chloride, Applied Microbiology, 12. No. 2, 132-137.

42.   Huang, W.-C., Lee, T.-J., Hsiao, C.-S., Chen, S.-Y.,   Liu, D.-M. Characterization and drug release behavior of chip-like amphiphilic chitosan-silica hybrid hydrogel for electrically modulated release of ethosuximide: An in vitro study Journal of Materials Chemistry 2011, 21(40), pp. 16077-16085.

43.   Chen, X., Liu, Z. A pH-Responsive Hydrogel Based on a Tumor-Targeting Mesoporous Silica Nanocomposite for Sustained Cancer Labeling and Therapy Macromolecular rapid communications 2016, 37(18), pp. 1533-1539.

44.   Radin, S., El-Bassyouni, G., Vresilovic, E.J., Schepers, E., Ducheyne, P. In vivo tissue response to resorbable silica xerogels as controlled-release materials Biomaterials 2005, 26(9), pp. 1043-1052.

45.   Ahola, M., Rich, J., Kortesuo, P., Kiesvaara, J., Seppala, J., Yli-Urpo, A. In vitro evaluation of biodegradable s-caprolactone-co-D,L-lactide/silica xerogel composites containing toremifene citrate International Journal of Pharmaceutics 1999, 181(2), pp. 181-191.

46.   K. Wong, G. Sun, X. Zhang, H. Dai, Y. Liu, C. He, K. W. Leong, HBPEI-g- chitosan, a Novel Gene Delivery System with Transfection Efficiency Comparable to Polyethylenimine in Vitro and after Liver Administration in Vivo, Bioconjugate Chem. 17 (2006) 152-158.

47.   I. Kitsou, E. Roussi, A. Tsetsekou, Synthesis of aqueous nanodispersed nanocrystalline ceria suspensions by a novel organic/inorganic precipitation method, Ceram. Int. 43 (2017) 3861-3865.

48.   Rao, R. R., Sathish, M., & Rao, J. R. (2021). Research advances in the fabrication of biosafety and functional leather: A way-forward for effective management of COVID-19 outbreak. Journal of Cleaner Production, 310, 127464.

49.   Arkas, M., Douloudi, M., Nikoli, E., Karountzou, G., Kitsou, I., Kavetsou, E., ... & Papageorgiou, M. (2022). Investigation of two bioinspired reaction mechanisms for the optimization of nano catalysts generated from hyperbranched polymer matrices. Reactive and Functional Polymers, 174, 105238.

50.   Panagiotopoulos, A. A., Karakasiliotis, I., Kotzampasi, D. M., Dimitriou, M., Sourvinos, G., Kampa, M., ... & Daskalakis, V. (2021). Natural polyphenols inhibit the dimerization of the SARS-CoV-2 main protease: the case of fortunellin and its structural analogs. Molecules, 26(19), 6068.\

51.   Wulff, N. H., Tzatzaris, M., & Young, P. J. (2012). Monte Carlo simulation of the spear-man-kaerber TCID50. Journal of clinical bioinformatics, 2(1), 1-5.

52.   L.Liz-Marzán, Nanometals: Formation and color, Mater.Today.7(2004)26–31.

53.   Arkas, M., Douloudi, M., Nikoli, E., Karountzou, G., Kitsou, I., Kavetsou, E., Korres D., et al. "Additional data on the investigation of the reaction mechanisms for the production of silica hyperbranched polyethylene imine silver nanoparticle composites." Data in Brief (2022): 108374.

54.   Monnery, B. D., Wright, M., Cavill, R., Hoogenboom, R., Shaunak, S., Steinke, J. H., & Thanou, M. (2017). Cytotoxicity of polycations: Relationship of molecular weight and the hydrolytic theory of the mechanism of toxicity. International journal of pharmaceutics, 521(1-2), 249-258.

55. Liang, Bing, Ming-Liang He, Zhong-Peng Xiao, Yi Li, Chuyan Chan, Hsiang-Fu Kung, Xin-Tao Shuai, and Ying Peng. "Synthesis and characterization of folate-PEG-grafted-hyperbranched-PEI for tumor-targeted gene delivery." Biochemical and biophysical research communications 367, no. 4 (2008): 874-880.

56. Abou Elmaaty, T.; Sayed-Ahmed, K.; Elsisi, H.; Ramadan, S.M.; Sorour, H.; Magdi, M.; Abdeldayem, S.A. Novel Antiviral and Antibacterial Durable Polyester Fabrics Printed with Selenium Nanoparticles (SeNPs). Polymers 2022, 14, 955. https://doi.org/10.3390/polym14050955.

57. Wang, W.-Y.; Yim, S.-L.; Wong, C.-H.; Kan, C.-W. Study on the Development of Antiviral Spandex Fabric Coated with Poly(Hexamethylene Biguanide) Hydrochloride (PHMB). Polymers 2021, 13, 2122. https://doi.org/10.3390/polym13132122.

58. Štěpánová, V.; Kelar, J.; Slavíček, P.; Chlupová, S.; Stupavská, M.; Jurmanová, J.; Černák, M. Surface modification of natural leather using diffuse ambient air plasma, Inter. J. Adhes. Adhesives 2017, 77, 198–203, https://doi.org/10.1016/j.ijadhadh.2017.05.004.

59. You, X.; Gou, L.; Tong, X. Improvement in surface hydrophilicity and resistance to deformation of natural leather through O_2/H_2O low-temperature plasma treatment. Appl. Surf. Sci. 2016, 360, 398–402, https://doi.org/10.1016/j.apsusc.2015.11.030.

60. Kim, Y.H. and G. Sun, 2001. Durable antimicrobial finishing of nylon fabrics with acid dyes and a quaternary ammonium salt. Text. Res. J., 71: 318-323.

61. Tatsuo, T., I. Masahiro, K. Kyoji and S. Yukio, 1989. Synthesis and antibacterial activity of copolymers having a quaternary ammonium salt side group. J. Applied Polymer Sci., 37: 2837-2843.